Korean J. Chem. Eng., 32(5), 980-992 (2015)
DOI: 10.1007/s11814-014-0274-1

pISSN: 0256-1115
eISSN: 1975-7220

Kinetics and modeling of methyl methacrylate graft copolymerization in the presence of natural rubber latex

Tanita Sirirat*, Terdthai Vatanatham*, Nanthiya Hansupalak*, Garry Llewellyn Rempel, and Wanvimon Arayapranee***,†**

*Department of Chemical Engineering, Kasetsart University, Bangkok 10900, Thailand
**Department of Chemical Engineering, University of Waterloo, Ontario N2L 3G1, Canada
***Department of Chemical and Material Engineering, Rangsit University, Phathum Thani 12000, Thailand
(*Received 25 May 2014 • accepted 11 September 2014*)

Abstract−A graft copolymerization model for using cumene hydroperoxide/tetraethylenepentamine (CHPO/TEPA) as a redox initiator was developed to describe the grafting of methyl methacrylate onto natural rubber latex as a core-shell particle. The model allows estimating the effects of the initiator concentration, monomer-rubber weight ratio, and temperature on the properties of graft product, e.g., % grafting efficiency and the % monomer composition in the graft copolymer and free polymer. The rate expressions of polymer chain formation are developed by taking into account a reduction of CHPO by TEPA and a population event of radicals between core/shell phases. The parameter estimation is performed to find the kinetic parameters. Validation with experimental results demonstrates a good applicability of the proposed model. The model results reveal that the formation of grafted polymer chains rather form by the chain transfer reaction to rubber chains from homopolymer radicals and the initiation reaction of cumyloxy radicals to rubber chains.

Keywords: Core-shell Particle, Graft Copolymerization, Methyl Methacrylate, Modeling, Natural Rubber Latex

INTRODUCTION

As the awareness of environmental issues has significantly increased in the past few years, using renewable materials such as natural polymers and their derivatives is becoming a new societal trend. Natural rubber (NR) is considered a green polymer due to its reusable nature. It can readily be obtained in Thailand, the world's largest producer and exporter. Annually, the export of NR to overseas markets earns an income of approximately 2-3 hundred billion baht, which falls in the top five of all export values [1]. For more than a year, the prices of NR have been falling as the result of the fluctuation of world market demand, climate conditions, exchange rates, etc., resulting in a 31% decrease in Thailand's NR export value. Consequently, an attempt has been made to increase NR domestic consumption, which is usually 10-15% of all NR production. Adding value to NR is one of the options to significantly boost Thailand's rubber industry. With various outstanding properties, NR can be further improved to extend its limitations in many industrial applications [2,3], thus allowing NR to compete with synthetic rubber.

Graft copolymerization is an alternative to modifying the properties of natural polymers by incorporating new functional groups onto the natural polymer based on the desired application. This technique has been applied for various natural polymers such as cellulose, cow leather, wool fiber, NR, etc [4-8]. For example, grafting butyl acrylate onto cellulose enhances its thermal and chemical resistance properties and decreases the moisture absorption property of cellulose, providing the cellulosic functional polymer for different applications such as in the packaging and bioplastics industries [9]. Likewise, grafting vinyl monomer onto NR can improve some physical properties of NR, such as mechanical properties and resistance to thermal, solvent, and oil, depending on the type of grafting monomer [10,11]. There are a number of vinyl monomers used to graft with NR; however, methyl methacrylate (MMA) and styrene are the most suitable monomers for grafting with NR since they provide a high grafting level [12]. The graft copolymer of NR and either MMA or styrene is usually used as an impact modifier for polymer blending since MMA and styrene are easily compatible with various polymers such as polypropylene, polyvinyl chloride, or polystyrene [13-15]. Due to the higher polarity of MMA, the graft copolymer of NR latex as a core and MMA as a shell has outstanding application in adhesive fields, which can be utilized in the production of shoes and furniture and in paper processing, such as adhesive for leather shoe, heat resistant lasting adhesives, and polyvinyl chloride adhesive tape [16,17]. In addition, poly(MMA)-grafted NR can be alternatively used as a polymer-matrix for a composite polymer electrolyte containing titanium dioxide/lithium tetrafluoroborate. The polarity characteristics provided by poly(MMA) can serve as a conducting medium to transport lithium ions [18].

The grafting process of NR has been quantitatively studied for several years [19,20]. It is usually carried out via free radical emulsion polymerization. Kochthongrasamee et al. [21] grafted MMA onto NR latex using various types of redox initiators. They revealed that cumene hydroperoxide/tetraethylenepentamine (CHPO/TEPA)

†To whom correspondence should be addressed.
E-mail: wanvimon@rsu.ac.th

provides the greatest % of grafted NR and grafting efficiency (GE) with respect to *tert*-butyl hydroperoxide/tetraethylenepentamine and potassium persulfate/sodium thiosulfate, indicating a higher efficiency of CHPO/TEPA over the others. The higher efficiency of CHPO/TEPA is due to the high hydrophobicity of CHPO radicals being concentrated on the NR surface to initiate graft copolymerization, leading to a high GE. Even though the process of grafting MMA onto NR has been applied for commercial purposes in industry, e.g., Regitex located in Japan, and has recently been extended into pilot plant production in Southern Thailand [22], its modeling and polymerization kinetics, which are required for efficient scale up and process design, have received little attention.

A number of reports [7,23,24] have appeared on a kinetic expression describing the relationship between the polymerization rate and grafting variables, such as initiator and monomer concentrations. Nevertheless, those rate expressions only provide information at the initial point. In fact, for grafting NR, most monomers in the system polymerize to form free polymeric radicals (homopolymer radicals) during the first 2-3 hours of reaction [25]. Thereafter, the polymeric radicals chemically bind to the backbone of NR, yielding a graft copolymer. As a result, both graft copolymer and free polymer (homopolymer) are produced during the reaction. Therefore, the information available at the initial point of the reaction might be insufficient to control the properties of the graft product, which is primarily formed 2-3 hours after the start of the polymerization. In addition, a literature search on grafting NR revealed that there is lack of a mathematical model for controlling graft product properties, e.g., the relationship between the GE describing how much monomer grafted onto NR and reactant concentration, as well as the relationship between the GE and time. Knowledge of this kinetic relationship is helpful for industrial production when maximizing the yield of the graft product, controlling its structure, and minimizing reactants and time required. Although some reports have proposed a mathematical model for grafting between a vinyl monomer and various types of backbone polymers [26-28], as yet none has been presented for NR.

We have developed a mathematical model for the batch emulsion graft copolymerization of MMA onto NR in the presence of CHPO/TEPA as a redox initiator. The proposed model allows the estimation of grafting efficiency during the reaction and provides additional information on the monomer compositions, e.g., % MMA composition in the graft copolymer and free polymer, which may make it possible to control the structural properties of graft copolymers quantitatively and qualitatively.

The proposed model was developed by modifying the model presented by Chern and Poehlein for the graft copolymerization of styrene onto polybutadiene seed latex particles using persulfate as an initiator [29]. Our proposed model was adjusted on the basis of redox initiator characteristics: CHPO/TEPA decomposes at the aqueous/particle interface due to its hydrophobic-hydrophilic properties [30]. The generated cumyloxy radicals behaving hydrophobically can penetrate into the monomer-swollen NR particles directly to induce the polymerization. A graft site (polyisoprene radical) can be produced by an initiation reaction of the cumyloxy radical and by a chain transfer reaction of growing radicals to NR. The grafting reaction primarily takes place near the surface of the NR particle or at the shell phase, owing to the surface-controlled process of grafting [31]. Because the growing polymer radicals can only move by a propagation event or by molecular motion [32], most growing polymer radicals are thus likely to be confined in the shell phase. As a result, the population of radicals is crowded near the surface of the NR particle, leading to the occurrence of a nonuniform distribution of radicals in the monomer-swollen NR particles.

Lastly, the proposed model is validated with experimental data

Table 1. Elementary reactions in free radical graft copolymerization of MMA onto NR using the CHPO/TEPA redox initiator

Mechanism	Rate equation	No.
I. Initiation reactions		
$ROOH+R'NH_2 \xrightarrow{k_i} RO^{\bullet}+R'NH^{\bullet}+H_2O$	$R_i=k_i[ROOH][R'NH_2]$	(1)
$RO^{\bullet}+MMA \xrightarrow{k_{im}} MMA^{\bullet}$	$R_{im}=k_{im}[RO^{\bullet}][MMA]$	(2)
$RO^{\bullet}+NR \xrightarrow{k_{ig}} NR^{\bullet}$	$R_{ig}=k_{ig}[RO^{\bullet}][NR]$	(3)
$NR^{\bullet}+MMA \xrightarrow{k_{gm}} NR-MMA^{\bullet}$	$R_{gm}=k_{gm}[NR^{\bullet}][MMA]$	(4)
II. Propagation reactions of homopolymer and graft copolymer		
$MMA^{\bullet}+MMA \xrightarrow{k_p} PMMA^{\bullet}$	$R_{p1}=k_p[MMA^{\bullet}][MMA]$	(5)
$NR-MMA^{\bullet}+MMA \xrightarrow{k_p} NR-PMMA^{\bullet}$	$R_{p2}=k_p[NR-MMA^{\bullet}][MMA]$	(6)
III. Chain transfer reactions		
$PMMA^{\bullet}+NR \xrightarrow{k_g} NR^{\bullet}+PMMA$	$R_{g1}=k_g[PMMA^{\bullet}][NR]$	(7)
$NR-PMMA^{\bullet}+NR \xrightarrow{k_g} NR^{\bullet}+NR-PMMA$	$R_{g2}=k_g[NR-PMMA^{\bullet}][NR]$	(8)
$MMA^{\bullet}+NR \xrightarrow{k'_g} NR^{\bullet}+MMA$	$R'_g=k'_g[MMA^{\bullet}][NR]$	(9)
$PMMA^{\bullet}+MMA \xrightarrow{k_{trm}} MMA^{\bullet}+PMMA$	$R_{trm1}=k_{trm}[PMMA^{\bullet}][MMA]$	(10)
$NR-PMMA^{\bullet}+MMA \xrightarrow{k_{trm}} MMA^{\bullet}+NR-PMMA$	$R_{trm2}=k_{trm}[NR-PMMA^{\bullet}][MMA]$	(11)
IV. Termination reactions		
$PMMA^{\bullet}_n+PMMA^{\bullet}_m \xrightarrow{k_t} PMMA_{n+m}$	$R_{t1}=k_t[PMMA^{\bullet}_n][PMMA^{\bullet}_m]$	(12)
$NR-PMMA^{\bullet}_n+PMMA^{\bullet}_m \xrightarrow{k_t} NR-PMMA_{n+m}$	$R_{t2}=k_t[NR-PMMA^{\bullet}_n][PMMA^{\bullet}_m]$	(13)

under various conditions.

MATHEMATICAL MODELING

1. Kinetic Mechanism

A reaction scheme for graft copolymerization of vinyl monomers onto NR latex induced by the CHPO/TEPA redox system has been presented by Arayapranee and Rempel [25]. It involves the following basic reactions: chain initiation, propagation of free polymer and graft copolymer chains, chain transfer to monomer and NR, and termination of polymer chains. The possible reaction steps are summarized in Table 1. In this system of seeded emulsion polymerization, there are monomer-swollen NR particles which are emulsified with surfactant in a continuous phase of water at the beginning of reaction. CHPO being hydrophobic primarily dissolves in the monomer-swollen NR particles, whereas the hydrophilic TEPA dissolves in the aqueous phase [33]. The interaction of CHPO/TEPA (oxidant/reductant) at the aqueous/monomer-swollen NR particle interface generates cumyloxy radicals (RO$^{\bullet}$) according to Eq. (1). The cumyloxy radicals could penetrate into monomer-swollen NR particles to interact with not only the MMA monomer but also the NR chains, yielding MMA radicals (MMA$^{\bullet}$) or polyisoprene radicals (NR$^{\bullet}$, called a graft site) as shown in Eqs. (2) and (3), respectively. The generated MMA$^{\bullet}$ are further added to MMA monomer, producing free poly(MMA) radicals (PMMA$^{\bullet}$). Likewise, the NR$^{\bullet}$ can propagate with MMA monomer, providing graft macroradicals or grafted poly(MMA) radicals (NR–PMMA$^{\bullet}$). As the reaction proceeds, the MMA$^{\bullet}$, PMMA$^{\bullet}$, and NR–PMMA$^{\bullet}$ can transfer a radical to either monomer or NR according to Eqs. (7)-(11). At the same time, PMMA$^{\bullet}$ and NR–PMMA$^{\bullet}$ can undergo

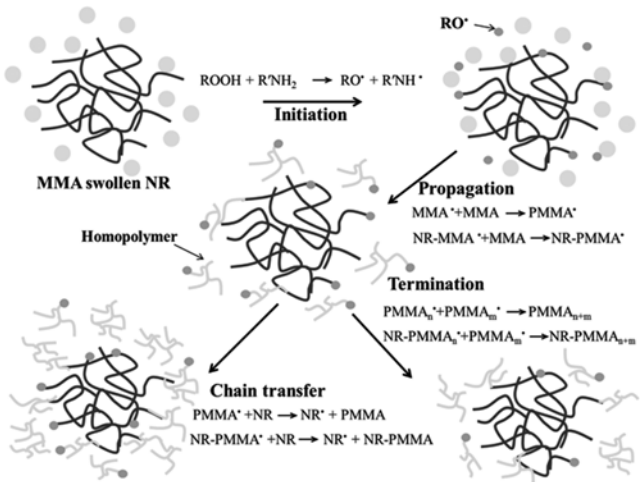

Scheme 1. Grafting mechanism.

Table 2. Mathematical model for grafting

Main equations	No.
Time-averaged grafting efficiency	
$\overline{GE}=\dfrac{\int_0^t[\text{Formation rate of graft copolymer chains}]dt}{\int_0^t[\text{Formation rate of total poly(MMA) chains}]dt}$	(14)
Formation rate of graft copolymer chains	
$\dfrac{d[\text{grafted chains}]}{dt}=\dfrac{d[NR^{\bullet}]}{dt}$	
$=k_{ig}[RO^{\bullet}][NR]+k_g\{[PMMA^{\bullet}]+[NR-PMMA^{\bullet}]\}[NR]+k'_g[MMA^{\bullet}][NR]$	(15)
$=k_{ig}[NR]_c(\bar{n}_c/N_{AV}v_p\varphi_c)(1-F_{np}-F_{nm})v_p\varphi_cN$	(15a)
$+k_g[NR]_c(\bar{n}_c/N_{AV}v_p\varphi_c)F_{np}v_p\varphi_cN$	(15b)
$+k'_g[NR]_c(\bar{n}_c/N_{AV}v_p)F_{nm}v_p\varphi_cN$	(15c)
Formation rate of total poly(MMA) chains	
$\dfrac{d[\text{poly(MMA) chains}]}{dt}=k_i[ROOH][R'NH_2]+k_{trm}\{[PMMA^{\bullet}]+[NR-PMMA^{\bullet}]\}[MMA]$	
$+k_g\{[PMMA^{\bullet}]+[NR-PMMA^{\bullet}]\}[NR]$	(16)
$=k_i[ROOH]\{[ROOH]+[R'NH_2]_0-[ROOH]_0\}$	(16a)
$+k_{trm}(\bar{n}/N_{AV}v_p)[MMA]_pv_pN$	(16b)
$+k_g[NR]_c(\bar{n}_c/N_{AV}v_p\varphi_c)F_{np}v_p\varphi_cN$	(16c)
Time-averaged monomer composition in graft copolymer	
$\overline{MG}=\dfrac{M_0xGE}{NR_0+M_0x}$	(17)
Time-averaged monomer composition in free polymer	
$\overline{MF}=\dfrac{M_0x(100-GE)}{NR_0+M_0x}$	(18)

termination by combination to form free poly(MMA) and graft copolymer, respectively, as shown in Eqs. (12)-(13). The main polymerization locus is thus near the surface of NR particles since any growing radicals can only move by molecular motion or by a propagation event [32]. As a result, the shell phase which is enriched in poly(MMA) is formed on the surface of the NR particle during the graft copolymerization. In addition, the buildup of PMMA$^{\bullet}$ near the NR particle surface would result in the formation of a nonuniform distribution of total radicals existing in the monomer-swollen NR particle. Hence, the number of total radicals in the monomer-swollen NR particle is separately considered between NR and poly (MMA) phases in the model development. The schematic of the grafting mechanism is displayed in Scheme 1. Three types of polymer chains are formed during the reaction: grafted poly(MMA) chains (graft copolymer), free poly(MMA) chains, and free NR (ungrafted) chains.

2. Kinetic Model Equations

According to the kinetic mechanism shown in Table 1, a mathematical model was developed and is expressed in Table 2. It provides the calculation of (1) time-averaged grafting efficiency, (2) %MMA composition in the graft copolymer, and (3) %MMA composition in the free polymer. The proposed model shown in Eqs. (14)-(16) is modified from the mathematical model developed by Chern and Poehlein who investigated the grafting of styrene onto polybutadiene using a persulfate initiator [29]. The assumptions adopted herein were derived from their work: (1) The radical reactivity only depends on the terminal units; for instance, the propagation reactions of grafted chains and free poly(MMA) chains have the same rate constants. (2) Free poly(MMA) and grafted poly(MMA) chains have identical chain lengths. (3) The reaction between free poly(MMA) and grafted poly(MMA)chains is insignificant in terms of undergoing cross-termination due to the chain length control of the chain transfer reactions. (4) The distribution coefficients of MMA between the core and shell phases are unity. (5) The number of latex particles remains constant.

Since the GE is the fraction of poly(MMA) grafted onto NR with respect to the total MMA conversion, the model was developed by considering the formation of graft copolymer chains and total poly

Table 3. Expressions for parameters appearing in Eqs. (14)-(18)

Equations	No.	Ref.
$F_{nm}=\dfrac{k_{trm}[MMA]_p}{k_p[MMA]_p+k_{trm}[MMA]_p+\dfrac{k_i[ROOH]\{[ROOH]+[R'NH_2]_0-[ROOH]_0\}N_{AV}}{N\bar{n}}}$	(19)	Modified from ref. 29
$F_{np}=\dfrac{k_p[MMA]_p}{k_p[MMA]_p+k_{trm}[MMA]_p+\dfrac{k_i[ROOH]\{[ROOH]+[R'NH_2]_0-[ROOH]_0\}N_{AV}}{N\bar{n}}}$	(20)	Modified from ref. 29
$[MMA]_p=\dfrac{M_0(1-x)}{\dfrac{M_0}{\rho_m}+\dfrac{NR_0}{\rho_r}}\times\dfrac{1000}{MW_m}$	(21)	35
$[NR]_c=\dfrac{NR_0}{\dfrac{M_0}{\rho_m}+\dfrac{NR_0}{\rho_r}}\times\dfrac{1000}{MW_r}$	(22)	35
$N=\dfrac{NR_0}{\rho_r v_r v_w}$	(23)	This work
$x=At+\dfrac{1}{C+\dfrac{B}{t}}$	(24)	This work
where $A=-(4.97 \text{ to } 12.38)\times10^{-5}$, B=26 to 94, and C=0.97 to 1.1 at t=0 to 480 min		
$\bar{n}=\left[\dfrac{N_{AV}}{Nk_p(1-x)}\right]\dfrac{dx}{dt}$	(25)	29
$\bar{n}_s=\bar{n}P_i\dfrac{\int_0^{(r_s-r_c)/r}\rho(z)dz}{\int_0^{r_s/r}\rho(z)dz}+\bar{n}(1-P_i)(1-\varphi_c)$	(26)	29
$\rho(z)=e^{-1.4259-4.3787z}$	(27)	32
$P_i=\dfrac{\rho_a}{\rho+k_{trm}[MMA]_p\bar{n}}$	(28)	29
$\rho=\rho_a+\alpha k_d\bar{n}$	(29)	39
$\rho_a=\dfrac{k_i[ROOH]\{[ROOH]+[R'NH_2]_0-[ROOH]_0\}N_{AV}}{N}$	(30)	This work

(MMA) chains as shown in Eq. (14). The formation rate of graft copolymer chains is presumably equal to the formation rate of polyisoprene radicals (Eq. (15)). According to the mechanism, the polyisoprene radicals can be produced by the attack of cumyloxy radicals on the NR chains (Eq. (3)), and the chain transfer to NR from MMA$^{\bullet}$, PMMA$^{\bullet}$, and NR−PMMA$^{\bullet}$ (Eqs. (7)-(9)). Note that, Eq. (3) is not included in the Chern and Poehlein model [29], which used persulfate as an initiator, because of the hydrophilicity of persulfate radicals. Typically, persulfate molecules decompose in the aqueous phase of the emulsion system, generating persulfate radicals. These persulfate radicals favorably attack the monomer in the aqueous phase, becoming oligomeric radicals. Afterward, these oligomeric radicals penetrate into the latex particles to further initiate polymerization [34]. The formation rate of the total poly(MMA) chains consisting of free poly(MMA) chains and grafted poly(MMA) chains can be written as shown in Eq. (16). This is represented by the summation of the formation rate of cumyloxy radicals (Eq. (16a)), the formation rate of MMA$^{\bullet}$ generated by chain transfer to the monomer (Eq. (16b)), and the formation rate of NR$^{\bullet}$ generated by chain transfer of PMMA$^{\bullet}$ and NR−PMMA$^{\bullet}$ to NR (Eq. (16c)). The subscript 0 represents the initial values.

3. Model Parameters

Table 3 shows the expressions for the calculation of the parameters in Eqs. (14)-(16). F_{mm} and F_{np} are the fraction of MMA$^{\bullet}$ and PMMA$^{\bullet}$ in the monomer-swollen particle, respectively. Both parameters are modified by considering the monomer-swollen particle consisting of cumyloxy radicals, MMA$^{\bullet}$, and PMMA$^{\bullet}$, including PMMA$^{\bullet}$ grafted on the NR chains.

The total number of radicals in the monomer swollen particle, $\bar{n}$, cannot be calculated via the Stockmayer-O'Toole solution [36,37], which was developed for emulsion polymerization, due to the very different glass transition temperature and molecular weight of the NR/poly(MMA) phases. In the proposed model, $\bar{n}$ is determined using curve fitting of the conversion-time data [38]. Since the distribution of growing radicals is nonuniform, the number of radicals in the latex particle is separately considered between the core and shell phases. Therefore, the number of radicals in the shell phase ($\bar{n}_s$) is written as a radical distribution profile, $\rho(z)$, which is relative to the particle radius (z) [29,32]. The difference between $\bar{n}$ and $\bar{n}_s$ at a particular time is the number of radicals present in the core phase ($\bar{n}_c$).

The calculation of grafting efficiency in Eq. (14) requires values of k_i, k_p, k_{trm}, k_g, k_{ig} and k'_g. The values for k_i, k_p, and k_{trm} were obtained by performing homopolymerization of MMA with CHPO/TEPA as an initiator, since those values have not been previously reported for this system. The k_i is determined according to Orr and Williams, who investigated the reaction of isopropyl cumene and tertiary butyl cumene hydroperoxides and iron (II) in aqueous solution in the absence of oxygen [40]. In this work, the residual of CHPO concentration ([*ROOH*]) is measured at a particular time by an iodometric method [41] rather than by the iron (II) concentration. On integrating Eq. (16a) with time, k_i can be obtained from the slope of the curve.

k_p is determined during interval II of the polymerization in which the rate of emulsion polymerization (R_p) is constant according to Harkin's theory [42]. R_p is a function of the MMA concentration in the particle and the number of poly(MMA) particles. R_p is obtained from the conversion-time data of the MMA homopolymerization. The MMA concentration in the particle is calculated according to the equation proposed by Burnett and Lehrle [43] in which the monomer-polymer ratio parameter needs to be measured according to the method of Herfeld and co-workers [44]. The number of poly(MMA) particles is calculated according to the work of Ramirez et al. [45]. Moreover, k_{trm} is determined by the so-called Mayo's procedure in which a plot of the inverse of the number-average degree of polymerization versus R_p yields k_{trm}/k_p as the y-intercept of the curve [46].

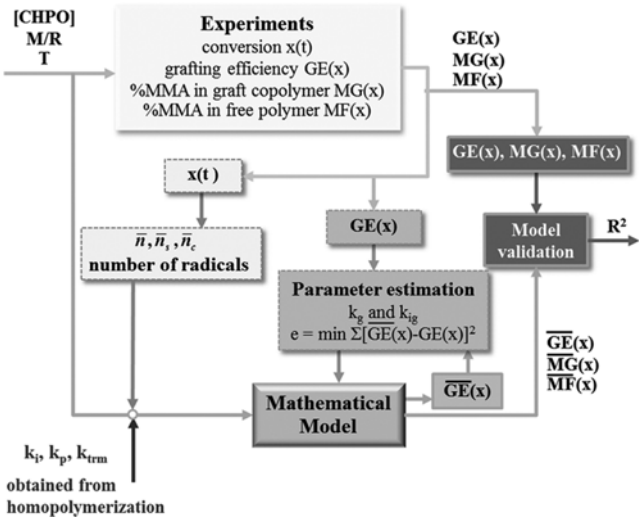

Scheme 2. Proposed model scheme for graft copolymerization.

The values of k'_g and k_g depend on the reactivity of the MMA radical and poly(MMA) radical, respectively. It was found that the reactivity of a styryl radical is approximately ten-times higher than that of a polystyryl radical, as reported by Chern and Poehlein [29]. Consequently, the value of k'_g is ten-times that of k_g. Therefore, there are only two unknown parameters, the k_{ig} and k_g grafting rate constants, which need to be determined by parameter estimation. The proposed model was solved using MATLAB version R2009b. The schematic of model estimation is summarized in Scheme 2, which can be described as follows:

(i) Perform polymerization experiments to characterize the polymer properties at the desired time (t), e.g., MMA conversion (x), GE, %MG, and %MF.

(ii) Use curve fitting of x(t) data (Eq. (24)) to calculate $\bar{n}$ and $\bar{n}_s$ according to Eqs. (25) and (26). Note that $\bar{n}_c$ is different from $\bar{n}$ and $\bar{n}_s$.

(iii) Perform parameter estimation to determine k_g and k_{ig} at various temperatures studied by fitting the model results ($\overline{GE}$) to the experimental data using a least squares error approach.

(iv) Input all kinetic and physical parameters, which are obtained from steps (ii) and (iii), and rate constants (k_i, k_p, k_{trm}) obtained from performing homopolymerization, into the model (Eqs. (14)-(18)) and estimate $\overline{GE}$, $\overline{MG}$, and $\overline{MF}$.

(v) Validate the model with the experiment data.

The values of kinetic and physical parameters used in this work are summarized in Table 4.

Table 4. Kinetics and physical parameters obtained in the current work or taken from literature

Parameter	Value or expression	Unit	Ref.
k_g	0.91 @ 40 °C	$L \cdot mol^{-1} \cdot min^{-1}$	This work
	2.61 @ 60 °C		
k'_g	9.1 @ 40 °C	$L \cdot mol^{-1} \cdot min^{-1}$	This work
	26.1 @ 60 °C		
k_{ig}	189 @ 40 °C	$L \cdot mol^{-1} \cdot min^{-1}$	This work
	242 @ 60 °C		
k_i	$3.48\times10^{6}\times e^{[-52.99\ (kJ/mol)/RT\ (K)]}$	$L \cdot mol^{-1} \cdot min^{-1}$	This work
k_p	$2.04\times10^{9}\times e^{[-31.05\ (kJ/mol)/RT\ (K)]}$	$L \cdot mol^{-1} \cdot min^{-1}$	This work
k_{trm}/k_p	5.7×10^{-5} @ 30 °C	-	This work
	6.9×10^{-5} @ 50 °C		
	8.3×10^{-5} @ 70 °C		
	$0.0015\times e^{[-8.25\ (kJ/mol)/RT\ (K)]}$		
k_d	0	min^{-1}	Neglected
MW_r	68.12	$g \cdot mol^{-1}$	-
MW_m	100.12	$g \cdot mol^{-1}$	-
r	200	nm	32
r_c	66	nm	This work
α	0	-	Neglected
ρ_m	0.92 (for G1-4)	$g \cdot cm^3$	60
	0.9 (for G5-8)		
ρ_r	0.91	$g \cdot cm^3$	-

MATERIALS AND METHODS

1. Materials

The NR latex used in this work was commercial high-ammonia grade containing 60% dry rubber content (DRC). The NR latex was obtained from *Hevea brasiliensis* supplied by Thai Hua Rubber Public Company Ltd., Rayong, Thailand. MMA monomer (Reagent grade ≥99%; Aldrich, USA) was purified by washing with a 10% aqueous solution of sodium hydroxide (~99%; Caledon, Canada) followed by deionized water until neutral. Sodium lauryl sulfate (SDS, ≥99%; Aldrich, Japan) was used as received as a surfactant, isopropanol (99.5%; EMD, Canada) as a stabilizer, potassium hydroxide (KOH, ~85%; BDH Inc., Canada) as a buffer, and CHPO (~80%; Aldrich, USA) as an initiator of the redox initiator system containing TEPA (~85%; Aldrich, USA) as an activator agent. Deionized (DI) water was used for all solution preparations.

Table 5. Emulsion graft polymerization recipes

Ingredients	Amount
NR latex (g)	40
M/R	0.25-0.75
CHPO (phr)[a]	1-2
(CHPO : TEPA=1 : 1)	
KOH (g)	0.12
SDS (g)	0.36
Solid content (%)	20
T (°C)	40-60
t (min)	0-480

[a]Initiator amount in parts per hundred NR

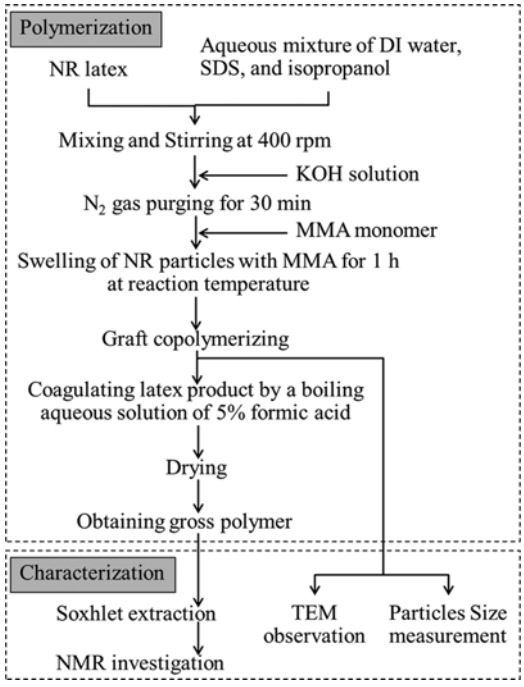

Fig. 1. Polymerization procedure.

2. Graft Copolymer Preparation and Characterization

A batch emulsion graft copolymerization was performed in a 500 mL Pyrex glass reactor, which was equipped with a reflux condenser, a stirrer, and a nitrogen inlet tube and placed in a water temperature-controlled bath. The ingredients used are summarized in Table 5. The monomer-rubber ratio (M/R), amount of CHPO per hundred parts rubber, temperature (T), and reaction time were varied. Note that M/R varied from 0.25 to 0.75, which can be written in MMA concentration as 0.52-1.08 $mol \cdot L^{-1}$. Likewise, the amount of CHPO 1-2 phr is equal to 0.0095-0.027 $mol \cdot L^{-1}$ of CHPO concentration. The reaction time was varied up to 480 minutes. As a result, eight polymerization conditions are assigned to study the grafting kinetics and to verify the model. The polymerization procedure is given in Fig. 1. A number of experiments were carried out one by one under the same condition but varied in time. The gross polymer product consists of a graft copolymer, free NR, and free poly(MMA). The free NR and free poly(MMA) were removed by soxhlet extraction. The free NR was washed out initially using a 60-80 °C boiling point petroleum ether for 24 h followed by a second extraction with a mixture of acetone/methyl ethyl ketone (50 : 50 v/v) for another 24 h to remove free poly(MMA). After soxhlet extraction, the product was dried to a constant weight in a vacuum oven at 50 °C, yielding graft copolymer. The monomer conversion, grafting efficiency, and %MMA composition in the graft copolymer and in the free polymer were determined gravimetrically according to the following relationships:

$$\text{Monomer conversion (x, \%)} = \frac{\text{weight of MMA polymerized}}{\text{weight of initial MMA}} \times 100 \quad (31)$$

Grafting efficiency (GE, %)

$$= \frac{\text{weight of MMA grafted}}{\text{weight of MMA polymerized}} \times 100 \quad (32)$$

%MMA in graft copolymer (MG, %)

$$= \frac{\text{weight of MMA grafted}}{\text{weight of gross polymer}} \times 100 \quad (33)$$

%MMA in free polymer (MF, %)

$$= \frac{\text{weight of free MMA}}{\text{weight of gross polymer}} \times 100 \quad (34)$$

The chemical grafting of MMA onto NR was characterized by ^{1}H NMR spectroscopy. The spectra were recorded on a Bruker 300 MHz spectrometer. The dried sample of graft copolymer was swollen in deuterated chloroform ($CDCl_3$).

The morphology of the graft copolymer was observed using a LEO 912AB transmission electron microscope (Carl Zeiss Inc., Germany) at 120 kV. The latex sample was diluted 400 times with DI water. A drop of 2% osmium tetroxide solution was dropped into the diluted solution of the latex sample and then left to sit overnight. Thereafter, a drop of stained solution was applied to a 400-mesh copper grid.

The size and size distribution of the NR particles were measured at 25 °C by Dynamic Light Scattering using a Nanotrac NPA 150 particle size analyzer (Betatek Inc., Canada). The particle size was reported as the number average diameter.

RESULTS AND DISCUSSION

1. Kinetics Parameters for MMA Homopolymerization

By observing the change in temperature over the range of 30-70 °C, the values of k_i, k_p, and k_{trm} obtained in this work can be summarized via an Arrhenius relation (Table 4), which yields a coefficient of determination (R^2) of ~0.98. Interestingly, our activation energy for the decomposition of CHPO by TEPA (53 kJ/mol) is lower than that of the thermal decomposition of CHPO in solution polymerization. Stannett and Mesrobian [47] studied the decomposition of CHPO in xylene at various concentrations of monostyrene and reported that the activation energy for the decomposition of CHPO over the temperature range of 73.5-110 °C was 101 kJ/mol. In addition, Forham and Williams [48] found that the decomposition of CHPO over the temperature range of 90-110 °C via a unimolecular fission process, presumably at the O-O bond, had an activation energy of approximately 127 kJ/mol. However, the value is greater than the decomposition of CHPO by ferrous ion (Fe^{2+}) for acrylonitrile solution polymerization over the temperature range of 0-25 °C (50 kJ/mol) [49]. This can be explained by the fact that a stronger electron donor, i.e., Fe^{2+}>TEPA, and the transfer of an electron to the O-O linkage from Fe^{2+} and TEPA have high activity to generate RO$^{\bullet}$ radicals over homolytic scission of the O-O bond thermally, providing the decomposition rate of CHPO of Fe^{2+}>TEPA>thermal. In addition, polymerization using a redox initiator can occur at low temperatures [50], resulting in a lower energy to decompose the O-O linkage.

For the propagation reaction, the value of the activation energy (31 kJ/mol) is close to the value reported by Soh [51] (29 kJ/mol), whose work involved a measurement of the propagation rate constant during interval III of the emulsion polymerization using a seeded emulsion technique for MMA polymerization initiated by persulfate over the temperature range of 40-60 °C. Nevertheless, our value is higher than that reported by Gilbert [52] (22.34 kJ/mol) for determination of critically evaluated propagation rate coefficients in free radical bulk polymerization induced by a pulsed-laser over the frequency range of 0.5-25 Hz and temperature range of −1 to 90 °C. Kunyuan et al. [53] studied the radical bulk polymerization of MMA initiated with organic peroxide-amine systems. They found that the peroxide-N, N-dimethyl-*p*-toluidine (DMT) systems gave higher rate of bulk polymerization of MMA than the organic hydroperoxide-DMT systems. They took the activation energy for propagation of MMA as 26.4 kJ/mol [54]. The propagation rate constant, generally found to have the same value in emulsion polymerization as in the corresponding bulk polymerization at high conversion, is a function of both monomer reactivity and radical reactivity. In addition, the apparently different values of a rate constant may be a consequence of experimental error, experimental conditions, or method of calculation [54].

The value of k_{trm}/k_p observed in the present work was in the range of 5.7-8.3×10^{-5} for the temperature range studied 30-70 °C (Table 4). On comparing to the literature, it was found that the observed value herein at 50 °C (6.9×10^{-5}) is slightly higher than that reported by Whang et al. (4-5×10^{-5}) who studied emulsion polymerization of MMA at 50 °C [55]. In addition, the observed value is also greater than that reported by van Berkel et al. (1.8-3×10^{-5}) whose work determined the value of k_{trm}/k_p for seeded emulsion polymerization using 0.1-3 mM of potassium persulfate concentration under the same temperature [56]. Moreover, the observed value in this work is close to the reported value of k_{trm}/k_p (5.15×10^{-5}) for bulk polymerization induced by azobis(isobutyronitrile) at 50 °C [57]. As mentioned above, the different initiators can be directly affected by the polymerization process and will also affect the polymerization rate.

2. Characterization and Morphology of Grafted NR

The ^{1}H NMR spectra of the NR before and after grafting are illustrated in Fig. 2. The peaks of NR are attributed to the olefinic pro-

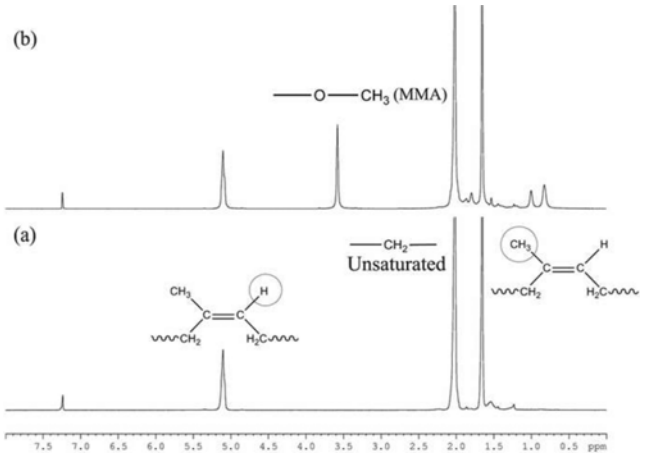

Fig. 2. ^{1}H NMR spectra of (a) NR and (b) poly(MMA)-g-NR (56% GE).

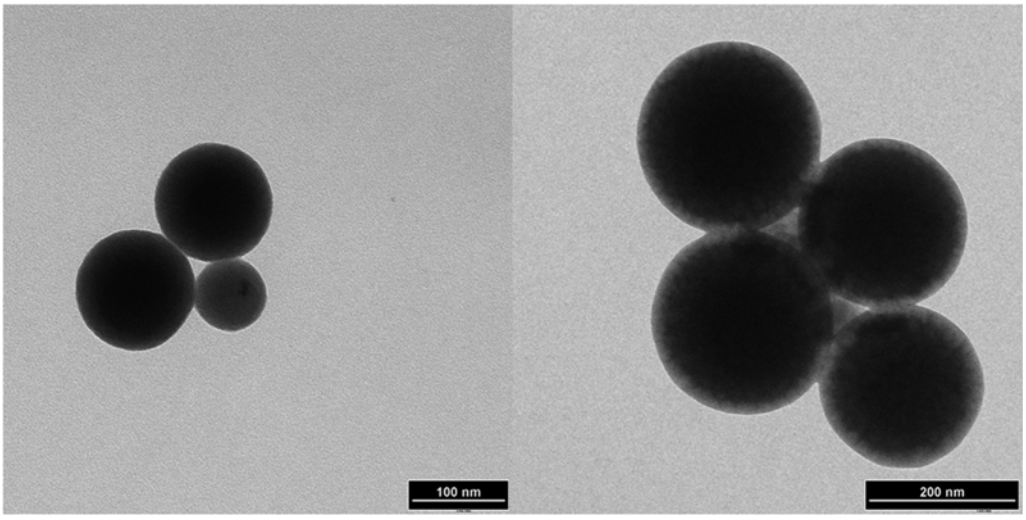

Fig. 3. TEM image of (a) NR and (b) poly(MMA)-g-NR (56% GE).

tons (=CH, at 5.1 ppm), the methylene protons (-CH_2-, at 2.02 ppm), and the methyl protons (-CH_3, at 1.66 ppm). After graft copolymerization (Fig. 2(b)), a new peak at 3.57 ppm was observed, which is attributed to the presence of the -OCH_3 of poly(MMA). This confirms that chemical grafting between MMA and NR occurred. In addition, the intensity of the peak at 5.1 ppm for the olefinic protons is constant, indicating no addition of MMA across the carbon-carbon unsaturated double bond of NR. Therefore, it can be deduced that the abstraction of an allylic hydrogen in the NR dominates the graft site initiation. A similar result has also been observed in grafting various types of vinyl monomers onto NR using CHPO/TEPA initiator (MMA and dimethylaminoethyl methacrylate by Oliveira et al. [8] and styrene by Kongparakul et al. [58]).

Fig. 3(a) illustrates the morphology of NR latex particles exhibiting a smooth spherical surface. After graft copolymerization, the heterogeneous core-shell structure with a nodular surface of grafted NR is observed as shown in Fig. 3(b). The dull domains represent NR particles as the core, whereas the brighter domains represent poly(MMA) as the shell. Clearly, the NR particle is completely encapsulated with poly(MMA) particles. The shell thickness is less than

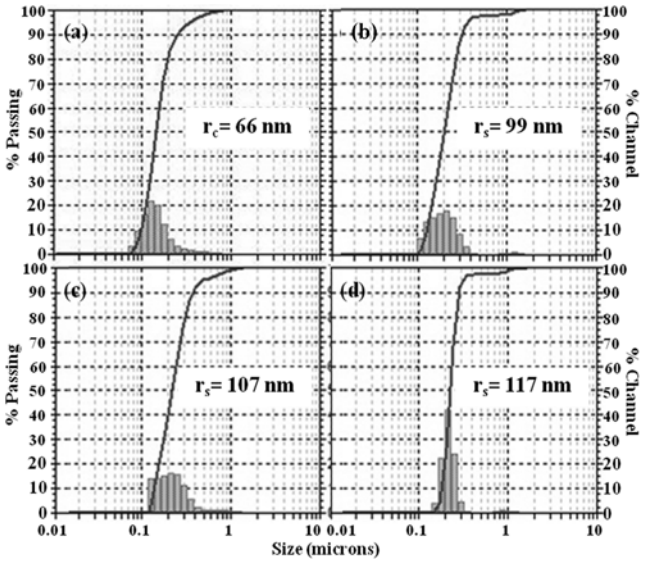

Fig. 4. Size distribution of (a) NR and poly(MMA)-g-NR with (b) 49% GE, (c) 56% GE, and (d) 64% GE.

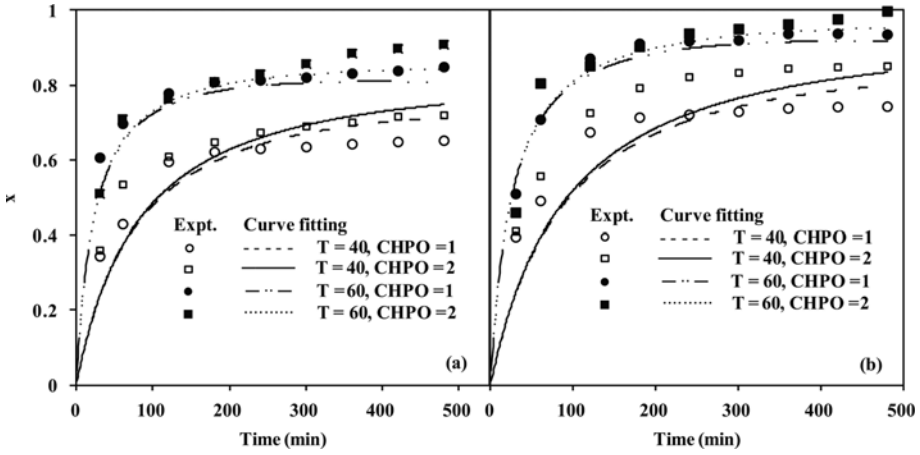

Fig. 5. Conversion-time profiles of poly(MMA)-g-NR: (a) M/R=0.25 and (b) M/R=0.75.

40 nm.

A particle size distribution of NR and grafted NR was observed. Fig. 4(a) shows a unimodal particle size distribution of NR particles with an average radius (r_c) of 66 nm. Typically, the size distribution of NR particles maintained with ammonia is in the radius range of 50 nm to 1 micron, depending on the age of the NR tree [59]. After the grafting process, the distribution peak of the grafted particles has shifted to the right-hand side of NR particles, as illus-

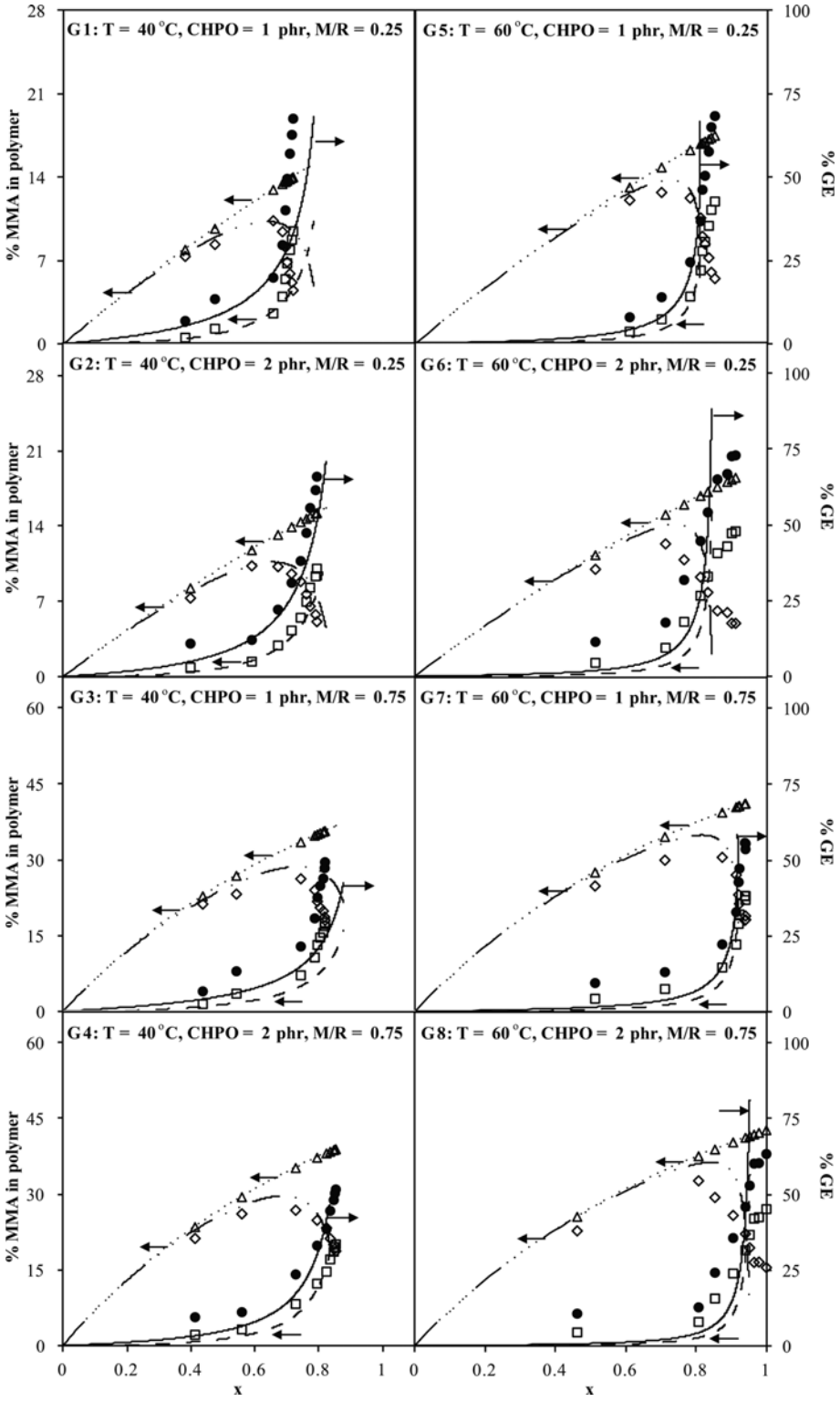

Fig. 6. Comparison of experimental results (symbols) and model predictions (lines) for variations of the GE (—, ●) and percentage of monomer in the graft copolymer (– –, □), in the free polymer (–··, ◇), and in the gross polymer (····, △) with conversion.

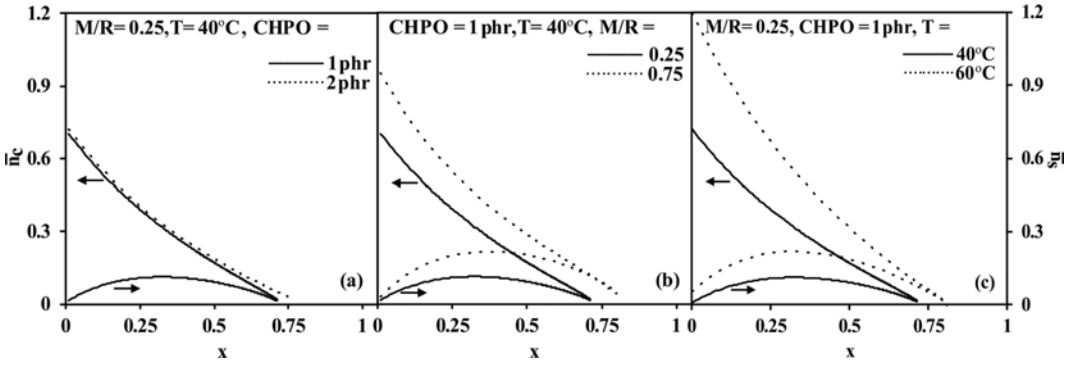

Fig. 7. The predicted number of radicals in core and shell phase: (a) effect of initiator, (b) effect of M/R, and (c) effect of temperature.

trated in Figs. 4(b)-(d). By increasing GE from 49 to 64%, the average radius of grafted NR (r_s) increases from 99 to 117 nm, indicating an increase in shell thickness of grafted NR from 33 to 51 nm.

3. Kinetics Study for Graft Copolymerization

The graft copolymerization of MMA onto NR is carried out under various experimental conditions to study the effect of the monomer-rubber weight ratio, initiator concentration, and reaction temperature. The monomer conversion, grafting efficiency, and % MMA composition in the free polymer and graft copolymer are measured at a particular time and presented in Figs. 5 and 6. The results, which have a similar trend for all experiments, show an increase of conversion with time up to 180 minutes before reaching a plateau. During the increase in conversion, the % MMA composition in the free polymer and graft copolymer and the GE also rise. Obviously, the % MMA composition in the free polymer is greater than that in the graft copolymer, indicating the formation of free poly(MMA) radicals upon grafted poly(MMA) radicals during this interval. Nevertheless, after approaching a plateau level of conversion, the consumption of free polymer in the system is apparently detected, whereas the formation of graft copolymer continuously increases, resulting in a steep increase in GE. This phenomenon indicates that most of the MMA monomer likely polymerized to form free poly(MMA) radicals during the early course of polymerization. Afterward, those poly(MMA) radicals are combined with polyisoprene radicals by a transfer reaction or by a termination reaction, yielding graft copolymer.

4. Parameter Estimation

The experimental GE-x data were fit with the model (Eq. (14)) to estimate the grafting rate constants (k_g and k_{ig}) using a least squares approach. The data used in the estimation were taken from experiments G4 and G8 operated at 40 and 60 °C, respectively. The best fit yields the grafting rate constants at a particular temperature, as reported in Table 4. According to the magnitude of k_{ig}, it can be concluded that the initiation reaction of cumyloxy radicals to NR chains has a significant effect on graft site initiation.

5. Model Validation

The estimated values of k_g and k_{ig} at 40 and 60 °C were used to verify the model for conditions G1-3 and G5-7, respectively. Fig. 6 shows a comparison of the model predictions for GE, %MMA composition in free polymer and graft copolymer to the experimental data under various conditions. The simulated results agree well with the experimental results, indicating good performance of the proposed model. Therefore, the kinetic parameters obtained from the parameter estimation and homopolymerization experiments can be used with confidence for prediction of the graft copolymer properties.

In addition, the proposed model is able to describe the influence of grafting variables, as expected. The observation shows that GE is predicted to increase when the amount of initiator is increased. An increase in initiator amount promotes the generation of MMA radical number. Therefore, the probability of radicals transfer to rubber to form graft site is raised, causing a larger of GE. The occurrence of more MMA radicals can be confirmed by the predicted total number of radicals in the core and shell phases. As can be seen in Fig. 7(a), $\bar{n}_c$ for 2 phr of initiator is more than that of 1 phr, even if $\bar{n}_s$ for both initiator concentrations is almost the same. An increased number of radicals in the core phase encourages the formation of graft site, thus giving a higher of GE.

With an increase in the monomer-rubber weight ratio from 0.25 to 0.75, the decrease of GE is apparent. In the presence of a low monomer concentration, nearly all of the monomer reacts with excess NR molecules due to a surface-controlled process of graft copolymerization. The contact area between the NR and monomer is large. Hence, it is easy for the monomer to diffuse and react with the NR chains. The GE then increases. In addition, an increase in the monomer-rubber weight ratio yields more MMA radicals, as can be seen in Fig. 7(b), in that both $\bar{n}_c$ and $\bar{n}_s$ increase. The greater number of radicals leads to the higher amount of polymer produced for both graft copolymer and free polymer, as shown in Fig. 6. For example, on comparing experiment G1 and G3 at highest conversion, % MMA in gross polymer, in graft copolymer, and in free polymer increases with increasing the monomer-rubber weight ratio. For G1 the % MMA in graft copolymer is larger than that of in free polymer, whereas the reverse trend is observed for G3. As a result, the GE of G3, which has higher monomer-rubber weight ratio, is lower.

An increase in the reaction temperature from 40 to 60 °C provides a higher GE. Polymerization under higher temperature induces a faster initiator decomposition rate, yielding a larger number of growing radicals in the system. This is confirmed by Fig. 7(c), where both $\bar{n}_c$ and $\bar{n}_s$ increase with increasing temperature. In addition, increasing the temperature also enhances the mobility of the molecular chains and decreases the viscosity of the system. Hence, those growing radicals can easily penetrate through the NR chain to form graft copolymer, resulting in a greater GE at higher temperatures.

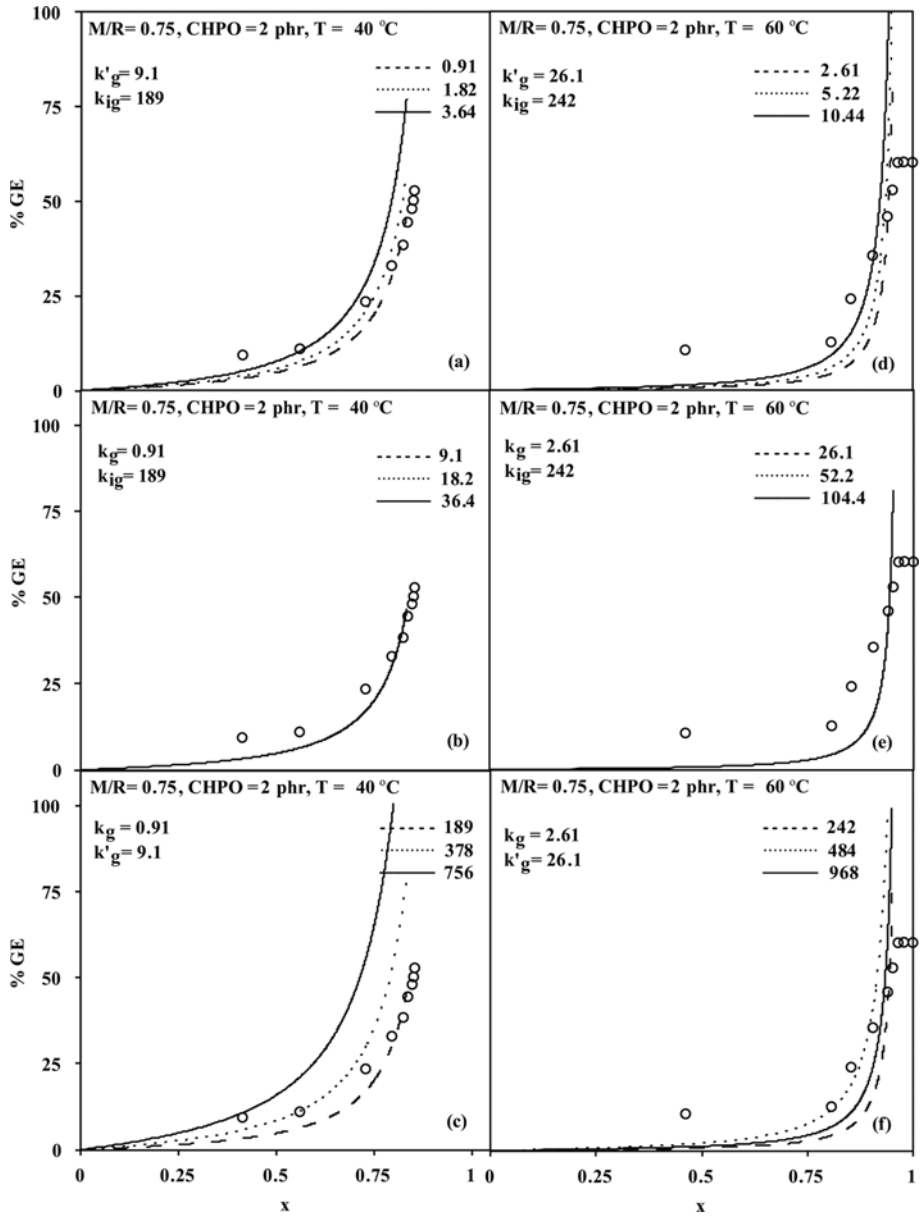

Fig. 8. The sensitivity of the model prediction to changes in k_g ((a) and (d)), ((b) and (e)), and ((c) and (f)).

According to the grafting mechanism, there are three graft site initiation steps (Eqs. (3), (7), (9)). Eqs. (7) and (8) are considered to be the same reaction, which involves the same poly(MMA) radicals. To estimate the relative importance of each graft site initiation step, a sensitivity analysis was performed for each temperature studied (40 and 60 °C), as shown in Fig. 8. The value of each grafting rate constant is varied by increasing it two-times for each increment, keeping the others constant at their optimal values. The dependence of the GE-x profiles on an increase of each grafting rate constant was observed. The model predictions are clearly sensitive to the change of $k_{ig}>k_g>k'_g$ for 40 °C and $k_{ig}>k_g>k'_g$ for 60 °C. An increase in k_{ig}, k_g, and k'_g of two-times induces an increase of approximately 57%, 37%, and 0.25% in the GE, respectively. This indicates that the initiation of cumyloxy radicals to the NR and the reaction of chain transfer to NR by poly(MMA) radicals play a major role in graft site initiation over the reaction of chain transfer to NR by MMA radicals.

CONCLUSIONS

A graft copolymerization model for using CHPO/TEPA as a redox initiator was successfully developed to describe grafting MMA onto NR latex as a core-shell particle. The model was developed by considering the characteristics of this redox initiator. Since it contains one hydrophobic and one hydrophilic component, the model has more complexity than using conventional persulfate as an initiator. As grafting takes place on the NR particle surface, a population event of radicals in the core/shell phases is also taken into account in the model development. The proposed model provides an estimation of the GE, %MMA composition in the graft copolymer

and free polymer, which are the key factors for controlling the graft copolymer properties. The model prediction can be applied throughout the period of the 8 hour experiment. The proposed model is also able to represent the influence of the grafting parameters well. In addition, a sensitivity analysis reveals that the initiation of cumyloxy radicals to the NR and the reaction of chain transfer to NR from poly(MMA) radicals play a major role in the graft site initiation. Therefore, this proposed model can be helpful for the production of the NR grafting process in choosing the suitable condition for the desired properties of the graft product by adjusting reactant amount and time required.

ACKNOWLEDGEMENTS

We gratefully acknowledge the financial support of Thailand Research Fund through the Royal Golden Jubilee Ph.D. Program grant # PHD/0098/2551, and appreciate the financial support of the Natural Sciences and Engineering Research Council of Canada (NSERC) and the Chemical Engineering Department, Faculty of Engineering, Kasetsart University and the Chemical Engineering Department of the University of Waterloo.

NOMENCLATURE

A, B, C, D : constant obtained from curve fitting
[CHPO] : concentration of cumene hydroperoxide [mol·L^{-1}_{water}]
F_{nm} : fraction of MMA$^{\bullet}$ in the monomer-swollen particle
F_{np} : fraction of PMMA$^{\bullet}$ which is free and grafted chains in the monomer-swollen particle
k_i, k_{im}, k_p, k_{trm}, k_t : rate constant for initiator decomposition, initiation, propagation, chain transfer, and termination reactions, respectively [$L \cdot mol^{-1} \cdot min^{-1}$]
k_d : first-order rate coefficient for loss of free radicals that leave the particle [min^{-1}]
k_{ig}, k_g, k'_g : grafting rate constant for cumyloxy radicals attacking NR and for transfer to NR by PMMA$^{\bullet}$ and MMA$^{\bullet}$, respectively [$L \cdot mol^{-1} \cdot min^{-1}$]
$\bar{n}$: total number of radicals per monomer-swollen particle
$\bar{n}_c$, $\bar{n}_s$: total number of radicals in core and shell phases
N : number of NR particles [L^{-1}_{water}]
N_{AV} : Avogadro's number [mol^{-1}]
$[NR]_c$: carbon-carbon double bond concentration per NR particle [$mol \cdot L^{-1}$]
NR_0 : initial mass of dry NR [g]
M_0 : initial mass of MMA [g]
MW_r : molecular weight of isoprene [$g \cdot mol^{-1}$]
MW_m : molecular weight of MMA [$g \cdot mol^{-1}$]
$[MMA]_p$: monomer concentration in monomer-swollen particle [$mol \cdot L^{-1}$]
P_i : the probability that any given radical is terminated by an initiator end-group
r : radius of reference particle [nm]
r_c, r_s : radii of the NR and graft copolymer particles [nm]
[TEPA] : concentration of tetraethylenepentamine [mol·L^{-1}_{water}]
v_p : volume of monomer-swollen particle [L]
v_r : volume of NR particle [cm^3]
v_w : initial volume of water [L]
X : fractional conversion
Z : normalized distance from particle surface to center

Greek Letters

α : fate parameter representing the fraction of exited radicals that reenter a particle
ρ : first-order rate coefficient for absorption of any radicals into a monomer-swollen particle [min^{-1}]
ρ_a : first-order rate coefficient for cumyloxy radicals entering a monomer-swollen particle [min^{-1}]
ρ_m : density of MMA [$g \cdot cm^3$]
ρ_r : density of dry NR [$g \cdot cm^3$]
$\rho(z)$: profile of radical distribution in the monomer-swollen particle
φ_c : the volume fraction of the core (NR) phase

REFERENCES

1. www2.ops3.moc.go.th (15 August 2013).
2. Y. C. Ko and G. Park, *Korean J. Chem. Eng.*, **24**, 975 (2007).
3. A. A. El-Wakil, *Polym. Plast. Technol. Eng.*, **46**, 661 (2007).
4. V. K. Thakur, M. K. Thakur and R. K. Gupta, *Carbohyd. Polym.*, **98**, 820 (2013).
5. V. K. Thakur, M. K. Thakur and R. K. Gupta, *Carbohyd. Polym.*, **104**, 87 (2014).
6. K. A. Shaffei, A. B. Moustafa and W. S. Mohamed, *J. Appl. Polym. Sci.*, **109**, 3923 (2008).
7. R. Anbarasan, T. Vasudevan and A. Gopalan, *J. Mater. Sci.*, **35**, 617 (2000).
8. P. C. Oliveira, A. M. Oliveira, A. Garcia, J. C. S. Barboza, C. A. C. Zavaglia and S. M. C. Santos, *Eur. Polym. J.*, **41**, 1883 (2005).
9. V. K. Thakur, M. K. Thakur and R. K. Gupta, *Carbohyd. Polym.*, **97**, 18 (2013).
10. R. A. Bakar and M. S. Fauzi, *J. Chem. Chem. Eng.*, **6**, 962 (2012).
11. N. M. Claramma, N. M. Mathew and E. V. Thomas, *Int. J. Radiat. Appl. Instrum. Part C Radiat. Phys. Chem.*, **33**, 87 (1989).
12. E. M. Bevilacqua, *J. Polym. Sci.*, **24**, 292 (1957).
13. S. B. Neoh, A. R. Azura and A. S. Hashim, *Polym. Plast. Technol. Eng.*, **50**, 121 (2011).
14. K. Eawsuwan, *Natural rubber grafted styrene/methyl methacrylate as impact modifier for poly (vinyl chloride)*, Thesis, Chulalongkorn University (2003).
15. H. Liu, D. Zuo, H. Liu, L. Li, J. Li and W. Xu, *E-Polym.*, **10**, 1499 (2013).
16. www.regitex.jp/english/mg.html (15 August 2013).
17. G. N. Onyeagoro, *Acad. Res. Int.*, **3**, 387 (2012).
18. S. P. Low, A. Ahmad, H. Hamzah and M. Y. A. Rahman, *J. Solid State Electrochem.*, **15**, 2611 (2011).
19. W. Wongthep, S. Srituileong, S. Martwiset and S. Amnuaypanich, *J. Appl. Polym. Sci.*, **127**, 104 (2013).
20. E. Kalkornsurapranee, K. Sahakaro, A. Kaesaman and C. Nakason, *J. Elastomers Plast.*, **42**, 17 (2010).
21. T. Kochthongrasamee, P. Prasassarakich and S. Kiatkamjornwong, *J. Appl. Polym. Sci.*, **101**, 2587 (2006).
22. E. Kalkornsurapranee, K. Sahakaro, A. Kaesaman and C. Nakason, *J. Appl. Polym. Sci.*, **114**, 587 (2009).

23. A. S. Singha, A. Guleria and R. K. Rana, *Int. J. Polym. Anal. Ch.*, **18**, 1 (2013).
24. K. Songsing, T. Vatanatham and N. Hansupalak, *Eur. Polym. J.*, **49**, 1007 (2013).
25. W. Arayapranee and G. L. Rempel, *J. Appl. Polym. Sci.*, **93**, 455 (2004).
26. J.-Y. Park and O. O. Park, *Korean J. Chem. Eng.*, **11**, 221 (1994).
27. C. G. Gutierrez, D. A. Estenoz, L. M. Gugliotta, J. R. Vega and G. R. Meira, *Latin. Am. Appl. Res.*, **36**, 309 (2006).
28. L. Li, L. Wu, Z. Bu, C. Gong, B.-G. Li and K.-D. Hungerberg, *Macromol. React. Eng.*, **6**, 384 (2012).
29. C. S. Chern and G. W. Poehlein, *J. Polym. Sci. Part. A: Polym. Chem.*, **28**, 3073 (1990).
30. W. Kangwansupamonkon, C. M. Fellows, D. J. Lamb, R. G. Gilbert and S. Kiatkamjornwong, *Polymer*, **45**, 5775 (2004).
31. J. Zhao, H. Yuan and Z. Pan, *J. Appl. Polym. Sci.*, **53**, 1447 (1994).
32. C. S. Chern and G. W. Poehlein, *J. Polym. Sci. Part A: Polym. Chem.*, **25**, 617 (1987).
33. W. Liu, R. Zheng and Z. He, *Polym. Bull.*, **61**, 27 (2008).
34. C. S. Chern, *Prog. Polym. Sci.*, **31**, 443 (2006).
35. C. F. Lee and W. Y. Chiu, *J. Appl. Polym. Sci.*, **56**, 1263 (1995).
36. W. H. Stockmayer, *J. Polym. Sci.*, **24**, 314 (1957).
37. J. T. O'Toole, *J. Appl. Polym. Sci.*, **9**, 1291 (1965).
38. D. C. Sundberg, J. Arndt and M. Y. Tang, *J. Dispersion Sci. Technol.*, **5**, 433 (1984).
39. M. J. Ballard, D. H. Napper and R. G. Gilbert, *J. Polym. Sci. Polym. Chem. Ed.*, **22**, 3225 (1984).
40. R. J. Orr and H. L. Williams, *Can. J. Chem.*, **30**, 985 (1952).
41. Solvay Chemicals, *Determination of hydrogenperoxide concentration (0.1% to 5%) Technical Datasheet TDS XX-122*, Solvay Chemicals Inc., Brussels, Belgium (2004).
42. W. D. Harkins, *J. Am. Chem. Soc.*, **69**, 1428 (1947).
43. G. M. Burnett and R. S. Lehrle, *Proc. R. Soc. London, Ser. A.*, **253**, 331 (1959).
44. S. H. Herzfeld, A. Roginsky, M. L. Corrin and W. D. Harkins, *J. Polym. Sci.*, **5**, 207 (1949).
45. J. C. Ramirez, J. Herrera-Ordonez and H. Maldonado-Textle, *Polym. Bull.*, **53**, 333 (2005).
46. F. R. Mayo, *J. Am. Chem. Soc.*, **65**, 2324 (1943).
47. V. Stannett and R. B. Mesrobian, *J. Am. Chem. Soc.*, **72**, 4125 (1950).
48. J. W. L. Fordham and H. L. Williams, *J. Am. Chem. Soc.*, **72**, 4465 (1950).
49. J. W. L. Fordham and H. L. Williams, *J. Am. Chem. Soc.*, **73**, 1634 (1951).
50. I. Reetz, Y. Yagci and M. K. Mishra, in *Handbook of radical vinyl polymerization*, M. K. Mishra and Y. Yagci, Eds., Marcel Dekker, New York, 45 (1998).
51. S. K. Soh, *J. Appl. Polym. Sci.*, **25**, 2993 (1980).
52. R. G. Gilbert, *Pure Appl. Chem.*, **68**, 1491 (1996).
53. Q. Kunyuan, S. Li and F. Xinde, *Polym. Commun.*, **1**, 64 (1984).
54. G. Odian, *Principles of polymerization, 4th Ed.*, Wiley-Interscience, Hoboken, New Jersey, 270, 364 (2004).
55. B. C. Y. Whang, M. J. Ballard, D. H. Napper and R. G. Gilbert, *Aust. J. Chem.*, **44**, 1133 (1991).
56. K. Y. van Berkel, G. T. Russell and R. G. Gilbert, *Macromolecules*, **38**, 3214 (2005).
57. D. Kukulj, T. P. Davis and R. G. Gilbert, *Macromolecules*, **31**, 994 (1998).
58. S. Kongparakul, P. Prasassarakich and G. L. Rempel, *Eur. Polym. J.*, **45**, 2358 (2009).
59. A. Rouilly, L. Rigal and R. G. Gilbert, *Polymer*, **45**, 7813 (2004).
60. C. I. Kao, D. P. Gundlach and R. T. Nelsen, *J. Polym. Sci.*, **22**, 3499 (1984).